Synthesis of Helional by Hydrodechlorination Reaction in the Presence of Mono- and Bimetallic Catalysts Supported on Alumina

Oreste Piccolo [1],*, Iztok Arčon [2,3], Gangadhar Das [4], Giuliana Aquilanti [4], Andrea Prai [5], Stefano Paganelli [5,6], Manuela Facchin [5] and Valentina Beghetto [5,6,7]

1 Studio di Consulenza Scientifica (SCSOP), Via Bornò 5, 23896 Sirtori, Italy
2 Laboratory for Quantum Optics, University of Nova Gorica, Vipavska 13, SI-5000 Nova Gorica, Slovenia; iztok.arcon@ung.si
3 Department for Medium and Low Energy Physics, Institute Jožef Stefan, SI-1000 Ljubljana, Slovenia
4 Elettra, Sincrotrone Trieste, s.s. 14 km 163.5, 34149 Basovizza, Italy; gangadhar.das@elettra.eu (G.D.); giuliana.aquilanti@elettra.eu (G.A.)
5 Dipartimento di Scienze Molecolari e Nanosistemi, Università Ca' Foscari Venezia, Via Torino 155, 30172 Venezia, Italy; andrea.prai@studenti.unime.it (A.P.); spag@unive.it (S.P.); manuela.facchin@unive.it (M.F.); beghetto@unive.it (V.B.)
6 Consorzio Interuniversitario Reattività Chimica e Catalisi (CIRCC), Via Celso Ulpiani 27, 70126 Bari, Italy
7 Crossing S.r.l., Viale della Repubblica 193/b, 31100 Treviso, Italy
* Correspondence: orestepiccolo@tin.it; Tel.: +39-3939479870

Abstract: Hydrodechlorination reaction of 3-(benzo-1,3-dioxol-5-yl)-3-chloro-2-methylacrylaldehyde in the presence of different low metal content heterogeneous mono- or bimetallic catalysts was tested for the synthesis of the fragrance Helional® (3-[3,4-methylendioxyphenyl]-2-methyl-propionaldehyde). In particular, mono Pd/Al_2O_3, Rh/Al_2O_3 or bimetallic Pd-Cu/Al_2O_3, Rh-Cu/Al_2O_3 catalysts were tested in different reaction conditions from which it emerged that mono-Rh/Al_2O_3 was the best performing catalyst, allowing achievement of 100% substrate conversion and 99% selectivity towards Helional® in 24 h at 80 °C, p(H_2) 1.0 MPa in the presence of a base. To establish correlations between atomic structure and catalytic activity, catalysts were characterized by Cu, Rh and Pd K-edge XANES, EXAFS analysis. These characterizations allowed verification that the formation of Pd-Cu alloys and the presence of Cu oxide/hydroxide species on the surface of the Al_2O_3 support are responsible for the very low catalytic efficiency of bimetallic species tested.

Keywords: Helional®; selective hydrodechlorination; heterogeneous catalysis; XANES analysis; EXAFS analysis

1. Introduction

Many heterogeneous catalysts are commercially available on the market, but their performances, in terms of selectivity, activity, stability and cost, are often unsatisfactory or unsustainable. To find a suitable catalyst for a specific process, fulfilling all the desired characteristics, remains a challenging task. When heterogeneous catalysts are employed, metal leaching or poisoning may sometimes occur, making the catalyst recyclability impossible. In particular, when fine chemicals are prepared, catalyst leaching implies further costly purification steps to reduce to authorised levels the presence of metal contamination. Many procedures have been developed to overcome these drawbacks and to obtain efficient heterogeneous catalysts, among which impregnation of metals on a support is one of the simplest and most commonly employed protocols. Metallic species are dispersed on a pre-dried support by incipient wetness impregnation techniques in aqueous or non-aqueous solution, followed by calcination and activation [1]. Milder and less energy-consuming preparation methods are relevant targets in catalyst development, possibly avoiding the

use of water to limit metal leaching. An interesting example has been reported in a patent by Piccolo and coworkers describing a simple and efficient protocol for the preparation, at an industrial scale, of a heterogeneous rhodium catalyst with very low metal loading (0.18% Rh/Al$_2$O$_3$). This catalyst proved to be very active for the selective hydrogenation of alpha-beta-unsaturated carbonyl compounds [2]. The catalyst, prepared in tetrahydrofuran (THF) or in the greener cyclopentyl methyl ether (CPME) at very low concentrations also showed excellent activity in terms of selectivity and recyclability [2,3]. As far as the synthesis of fine chemicals is concerned, Rh/Al$_2$O$_3$ but also Pd/Al$_2$O$_3$ and bimetallic Pd-Cu/Al$_2$O$_3$ catalysts have been demonstrated to be very active and selective in the semi-hydrogenation of 3-hexyn-1-ol to (*Z*)-3-hexen-1-ol, a particularly important fragrance with an herbaceous note [4].

Focusing on the synthesis of odorants [5], we deemed it interesting to evaluate the efficiency of these heterogeneous catalysts for the preparation of Helional® (3-[3,4-methylendioxyphenyl]-2-methyl-propionaldehyde)]. Helional® is a high added-value fragrance employed in its racemic form in many perfumes for its green, floral (cyclamen), and marine fresh note, prepared at an industrial level by different strategies (Scheme 1). Specifically, Helional® is mainly prepared by crossed-aldol condensation between heliotropin (5-carboxyaldehyde-1,3-benzodioxol) (**I**), which is now a controlled substance, and propanal to obtain (**II**), followed by selective hydrogenation of the intermediate alkene formed (Scheme 1a) [6,7]. However, this methodology has a series of disadvantages, such as, for example, the fact that yields above 50–55% may not be achieved in the aldol condensation due to self-condensation of propionaldehyde and the reaction of this with (**II**), requiring costly purification steps to separate by-products from (**III**). Alternative methods foresee the synthesis of Helional® starting from the alkylation of 1,2-methylenedioxybenzene (MDB) (**IV**) with 2-methylprop-2-ene-1,1-diyl diacetate (**V**), followed by hydrolysis of 1-acetoxy-2-methyl-3-(3,4-methylendioxyphenyl)propene) (**VI**) to give the desired product (**III**) (Scheme 1b) [8–10]. Synthetic strategies reported above suffer further drawbacks such as the use of expensive or difficult-to-handle catalysts, the use of Lewis acids, and the use of expensive reagents such as methacrolein diacetate (**V**). An interesting and not well investigated alternative has been reported by Borzatta and coworkers starting from cheap and easily available 5-propanoyl-1,3-benzodioxol (**VII**) [11]. (**VII**) is reacted with the Vilsmeier reagent (1-chloro-*N*,*N*-dimethyl-methan-iminium chloride) (**VIII**) at temperatures ranging between 0–40 °C to obtain the unsaturated chloroaldehyde 3-(benzo-1,3-dioxol-5-yl)-3-chloro-2-methylacrylaldehyde (**IX**), which is then hydrodechlorinated to give (**III**) in the presence of 5% Pd/C and an organic or inorganic base (Scheme 1c) [11].
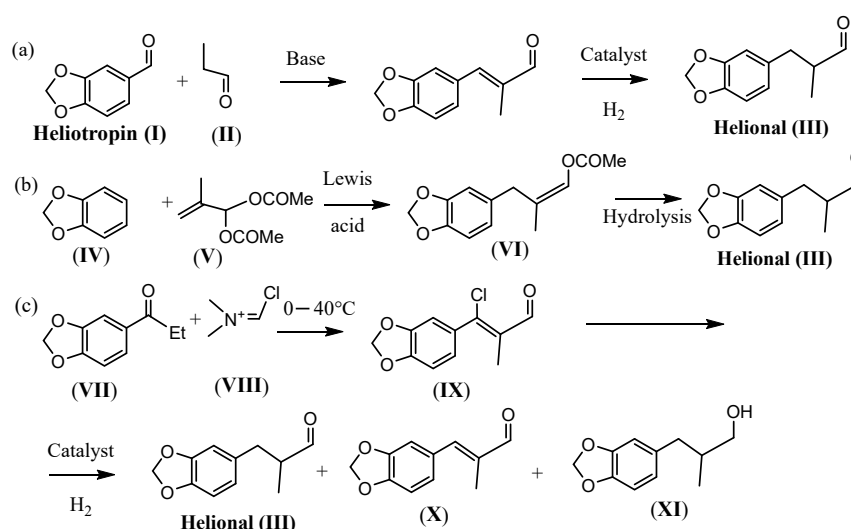
Scheme 1. Main protocols for the synthesis of Helional® (**III**). (**a**) preparation by crossed-aldol condensation; (**b**) preparation by alkylation of 1,2-methylenedioxybenzene (MDB); (**c**) preparation by Vilsmeier reaction and hydrodechlorination.

Within this panorama, the possibility to employ low metal content heterogeneous catalysts reported by Piccolo and collaborators [2–4] for the selective hydrodechlorination of α,β-unsaturated aldehydes such as (**IX**) appeared very challenging also for industrial applications.

Thus, in this paper the hydrodechlorination reaction of 3-(benzo-1,3-dioxol-5-yl)-3-chloro-2-methylacrylaldehyde (**IX**), for the selective synthesis of Helional® (**III**), has been reported in the presence of different low metal content heterogeneous mono-Pd/Al$_2$O$_3$ or Rh/Al$_2$O$_3$ and bimetallic Pd-Cu/Al$_2$O$_3$ and Rh-Cu/Al$_2$O$_3$ catalysts. Moreover, all catalysts tested were characterised by XANES and EXAFS before and after the hydrodechlorination reaction.

2. Results

The catalytic activity of the mono-Pd or Rh supported on Al$_2$O$_3$ and bimetallic Pd-Cu/Al$_2$O$_3$ or Rh-Cu/Al$_2$O$_3$ species were tested in different reaction conditions for the hydrodechlorination of 3-(benzo-1,3-dioxol-5-yl)-3-chloro-2-methylacrylaldehyde (**IX**) and data are reported below (Tables 1 and 2). The use of bimetallic species was investigated since Pd-Cu/Al$_2$O$_3$ or Rh-Cu/Al$_2$O$_3$ catalysts would allow to reduce the quantity of transition metal employed and consequently industrial costs.

Table 1. Hydrodechlorination of (**IX**) catalyzed by 0.3% Pd/Al$_2$O$_3$, or Pd-Cu/Al$_2$O$_3$ (0.18% Pd, 0.43% Cu) in the presence of different bases.

Run	Catalyst	Base	t (h)	Conv. (%) [a]	(X) (%) [a]	(III) (%) [a]	(XI) (%) [a]
1		Na$_2$CO$_3$	6	65	15	49	1
2		Na$_2$CO$_3$	24	98	3	74	21
3	Pd/Al$_2$O$_3$	TOA	6	81	6	56	19
4		TOA	24	95	3	62	30
5		TEA	6	88	11	72	5
6		TEA	24	100	1	83	16
7		TEA	6	7	3	4	n.d.
8	Pd-Cu/Al$_2$O$_3$	TEA	24	12	5	6	1
9 [b]		TEA	6	29	6	20	3
10 [b]		TEA	24	50	5	40	5

Reaction conditions: Substrate (**IX**): 20 mg (8.9 × 10^{-2} mmol); Catalyst: 0.3% Pd/Al$_2$O$_3$, 3.7 mg (8.9 × 10^{-5} mmol); (**I**)/Metal molar ratio: 1000/1; Solvent: 2-propanol (5 mL); T: 80 °C; p(H$_2$): 0.5 MPa; Base: 2 equivalents. The quantity of bimetallic catalyst was 5.3 mg (8.9 × 10^{-5} mmol); substrate/Pd molar ratio 1000/1. [a] Determined by GLC analysis in the presence of 8.9 × 10^{-3} mmol of isopropyl benzene as internal standard. [b] p(H$_2$): 1.0 MPa. n.d. = not determined.

Table 2. Hydrodechlorination of (**IX**) catalyzed by 0.18% Rh/Al$_2$O$_3$ or Rh-Cu/Al$_2$O$_3$ (0.19% Rh, 0.8% Cu) in the presence of different bases.

Run	Catalyst	Base	p(H$_2$) (MPa)	t (h)	Conv. [a] (%)	(X) (%) [a]	(III) (%) [a]	(XI) (%) [a]
1		Na$_2$CO$_3$	0.5	6	67	25	41	1
2	Rh/Al$_2$O$_3$	Na$_2$CO$_3$	0.5	24	85	3	72	10
3		Na$_2$CO$_3$	1.0	6	75	18	57	n.d.
4		TEA	1.0	24	100	1	99	n.d.
5		TEA	1.0	4	23	14	9	n.d.
6	Rh-Cu/Al$_2$O$_3$	TEA	1.0	16	43	12	28	3
7		TEA	1.0	24	68	9	51	8

Reaction conditions: Substrate (**IX**): 8.9 × 10^{-2} mmol; Catalyst: 8.9 × 10^{-5} mmol; (**I**)/Metal molar ratio: 1000/1; Solvent: 2-propanol (5 mL); T: 80 °C; Base: 2 equivalents. [a] Determined by GLC analysis in the presence of 8.9 × 10^{-3} mmol of isopropyl benzene as internal standard. n.d. = not determined.

*Catalytic Hydrodechlorination of 3-(Benzo1,3-dioxol-5-yl)-3-chloro-2-methylacrylaldehyde (**IX**)*

Preliminary experiments were carried out to verify the efficiency of mono- and bimetallic Pd based supported catalysts containing 0.3% or 0.18% quantities of palladium. Since the hydrodechlorination of (**IX**) leads to the formation of hydrochloric acid, first experiments were devoted to highlight the influence of different inorganic and organic bases [Na_2CO_3, trioctyl amine (TOA) and triethyl amine (TEA)] on the catalyst efficiency, and relevant data are reported in Table 1. Unless otherwise stated, reactions were carried out with a substrate/metal molar ratio of 1000/1 at 80 °C and 0.5 MPa p(H_2), in the presence of 2 equivalents of a base. Data reported in Table 1 are the mean values of at least three experiments.

After 6 h at 80 °C, in the presence of Na_2CO_3, the conversion was rather low (65%) and selectivity to (**III**) around 75%, with the formation of both the unsaturated product 3-(1,3-benzodioxol-5-yil)-2-methyl-propenal (**X**) (15%) and 3-(1,3-benzodioxol-5-yil)-2-methyl-propanol (**XI**) (1%) (run 1, Table 1). Increasing the reaction time to 24 h strongly increased substrate conversion (98%), although selectivity to (**III**) was almost equivalent to that achieved by 6 h (78%, compare runs 1 and 2), and the formation of alcohol (**XI**) also increased (run 2, Table 1). To verify if higher catalyst efficiency could be achieved substituting Na_2CO_3, insoluble in the reaction mixture, with a soluble organic base, further experiments were carried out in the presence of TOA or TEA. According to data reported in Table 1, it emerges that TOA gave no significant improvement as compared to Na_2CO_3 (compare runs 1–4, Table 1), while in the presence of less hindered TEA best results were obtained, affording 100% conversion of (**IX**) and 83% selectivity to (**III**) by 24 h (compare runs 3–6, Table 1).

Encouraged by the good results obtained with Pd/Al_2O_3, the activity of the bimetallic Pd-Cu/Al_2O_3 (0.18% Pd, 0.43% Cu) catalyst was also investigated. Bimetallic systems Pd-Cu/Al_2O_3 had been successfully employed in the hydrodechlorination of 4-chlorophenol [12]. In the same reaction conditions employed with Pd/Al_2O_3, the bimetallic specie gave very unsatisfactory results (runs 7–10, Table 1). At best, conversion was 50% and Helional® (**III**) was obtained in 80% selectivity after 24 h but at 1.0 MPa of hydrogen pressure (run 10, Table 1). A possible explanation for the lower activity of this catalytic species may be attributable to the formation of alloys that reduce the amount of active catalyst and to the presence of catalytically not active Cu(II) oxide/hydroxide species on the surface of the Al_2O_3 support (see Section 3).

Alternatively, 0.18% Rh/Al_2O_3 was tested for the catalytic hydrodechlorination of (**IX**), and results are reported in Table 2. In the same reaction conditions employed in the presence of 0.3% Pd/Al_2O_3 (run1, Table 1), Rh/Al_2O_3 gave comparable results (run 1, Table 2).

Moreover, increasing hydrogen pressure to 1.0 MPa, in the presence of 2 equivalents of TEA, allowed achievement of total conversion of (**IX**), with almost complete selectivity to (**III**) by 24 h (99%) (run 4, Table 2). Interestingly, no total hydrogenation by-product (**XI**) was detected in the reaction crude.

Finally, the activity of the bimetallic Rh-Cu/Al_2O_3 catalyst (0.19% Rh, 0.8% Cu) was also evaluated. Nevertheless, as for bimetallic Pd-Cu/Al_2O_3 species, also Rh-Cu/Al_2O_3 based catalyst showed very low performances compared to Rh/Al_2O_3 (entries 5–7, Table 2). Also in this case, catalytically not active Cu(II) oxide/hydroxide species are present on the surface of Al_2O_3, hindering the performance of the Rh active sites (see Section 3).

To gain further understanding on the nature of the catalysts and on the very low efficiency of bimetallic species, Pd/Al_2O_3, Rh/Al_2O_3, Cu/Al_2O_3, Pd-Cu/Al_2O_3, and Rh-Cu/Al_2O_3 were characterized, before and after catalytic reactions, by XANES and EXAFS (see Supplementary Materials).

3. Discussion

All the catalysts were previously studied by SEM and TEM electron microscopy, showing the lamellar structure of Al_2O_3 and highlighting the presence of metal nanoparticles on

the support surface with dimensions less than 10 nm. Moreover, SEM and TEM images demonstrated that the metal nanoparticles remain well dispersed on the support surface and do not aggregate after the reaction [4,13].

The Cu, Rh, and Pd K-edge XANES were used to monitor the valence state and local symmetry of Cu, Rh, and Pd cations in the Cu/Al_2O_3, Pd/Al_2O_3 $Pd-Cu/Al_2O_3$, Rh/Al_2O_3, and $Rh-Cu/Al_2O_3$ catalysts before and after the catalytic reaction. Different local environments of the investigated cation result in different K-edge profiles in the XANES spectra. Further, the Cu, Rh, and Pd K-edge EXAFS were used to determine the average local neighbourhood of Cu, Rh, and Pd cations in the Cu/Al_2O_3, $Rh-Cu/Al_2O_3$, and $Pd-Cu/Al_2O_3$ catalyst in the initial state and in the final state, after catalytic reaction. The analysis of the EXAFS spectra was performed with the Demeter (IFFEFIT) program package [14] in combination with the FEFF6 program code [15] for ab initio calculation of photoelectron scattering paths. Structural parameters of the average local Cu, Rh, and Pd neighbourhood (type and average number of neighbours, the radii and Debye–Waller factor of neighbour shells) are quantitatively resolved from the EXAFS spectra by comparing the measured EXAFS signal with model signal. Combined FEFF models are used, composed of neighbour atoms at distances characteristic for the expected Cu, Rh, and Pd oxide and metal species that may be present in the samples in the initial or final state or after catalytic reaction. For a comparison see [16–18]. The atomic species of neighbours are identified in the fit by their specific scattering factor and phase shift. Details of the XANES and EXAFS analyses are presented in the Supplementary Materials.

The Cu K-edge XANES results (Table S1) show that monometallic Cu/Al_2O_3, catalyst contains only Cu(II) cations octahedrally coordinated to oxygen atoms. The Cu valence state and local symmetry does not change during the catalytic reaction. Bimetallic $Rh-Cu/Al_2O_3$ catalyst also contains only Cu(II) species with the same local symmetry; however, during the catalytic reaction 15% of Cu cations are reduced to metallic form. Bimetallic $Pd-Cu/Al_2O_3$ catalyst contains a mixture of Cu cations in three valence states: 54% of Cu(II), 4% of Cu(I), and 42% of metallic Cu. During catalytic reaction, relative amounts of Cu(II) and Cu(I) species increased and relative amount of metallic Cu decreased.

The Cu EXAFS results (Table S2) show that Cu cations in monometallic Cu/Al_2O_3 and bimetallic $Rh-Cu/Al_2O_3$ catalyst in the initial state are coordinated with six oxygen atoms in the first coordination shell at two different distances, and Al and Cu are neighbours in more distant coordination shells. The distances to oxygen and Cu neighbours are characteristic for the local structures of Cu cations in Cu oxide/hydroxide species indicating that the samples contain a mixture of copper oxide/hydroxide species, in agreement with the Cu K-edge XANES result. The presence of two Al neighbours at about 3.1 Å clearly indicates that part of the Cu cations is directly attached to the Al_2O_3 framework forming Cu–O–Al bridges. So it is possible to conclude that the Cu(II) oxide/hydroxide species are highly dispersed on the Al_2O_3 support and tightly attached to its surface. During the catalytic reaction, the average structure of Cu oxide/hydroxide species in the monometallic Cu/Al_2O_3 is preserved. However, the average number of Al neighbours is significantly decreased, which indicates that about half of Cu–O–Al bridges are lost during the catalytic reaction.

In the bimetallic $Rh-Cu/Al_2O_3$ catalyst, the local structure around Cu cations changes significantly during the catalytic reaction. Part of Cu cations is reduced to metallic form, as already indicated by Cu XANES analysis, and form small Cu metallic nanoparticles with fcc crystal structure. The remaining part of Cu cations remains in the form of Cu(II) oxide/hydroxide species, but the Cu–O–Al bridges are lost.

The bimetallic $Pd-Cu/Al_2O_3$ catalyst contains a mixture of Cu metal nanoparticles with fcc crystal structure and Cu oxide/hydroxide species already present in the initial state, in agreement with the Cu K-edge XANES results. There are no Al neighbours in the second coordination shell, which indicates that there are no Cu–O–Al bridges present in the sample or that their amount is below the detection limit. During the catalytic reaction, the average local structure around Cu cations is mainly preserved. Only the coordination number of Cu neighbours in the second coordination shell in the metal fcc structure is significantly

increased, indicating that the average size of Cu metal nanoparticles is increased, and, according to the Cu K-edge XANES results, the relative amount of Cu metal species is slightly decreased, indicating a partial oxidation of Cu(0).

The Rh K-edge XANES analysis of the Rh/Al_2O_3 and $Rh-Cu/Al_2O_3$ catalyst in the initial state and in the final state after catalytic reaction indicate that the catalysts contain predominantly Rh oxide species and a small amount of Rh in the metallic form (Table S3). Relative amounts of metallic Rh species in the catalysts increase significantly during the catalytic reaction. The Rh EXAFS analysis (Table S4) shows that in all four samples, Rh cations are coordinated to oxygen neighbours at the distance of 2.03 Å, characteristic for Rh oxide, and Rh neighbours at 2.67 Å, characteristic for the nearest coordination shell in Rh metal. In the fresh monometallic Rh/Al_2O_3 sample, 4 oxygen atoms and only about 0.6 Rh neighbours were present, indicating that the sample contains predominantly Rh oxide species with about 10% of Rh in the metallic form. After the catalytic reaction, the average number of oxygen neighbours decreased to about 3 and the number of Rh neighbours increased to about 2. These results indicate that part of Rh oxide species is reduced to metallic form and relative amount of Rh metal species increased during the catalytic reaction. The same process was observed also for the bimetallic $Rh-Cu/Al_2O_3$ catalyst. After the catalytic reaction, the average number of oxygen neighbours decreased from 4 to about 2.5 and the average number of Rh neighbours increased from 1 to about 5, indicating that even higher amounts of Rh oxide species are reduced to the metallic form. The Rh EXAFS results are consistent with the Rh XANES results.

The Pd K-edeg XANES analysis of the Pd/Al_2O_3 and $Pd-Cu/Al_2O_3$ catalyst in the initial state and in the final state after catalytic reaction (Figure S6) indicate that the catalysts contain predominantly Pd in the metal form. The Pd EXAFS results (Table S5) reveal that fresh monometallic Pd/Al_2O_3 catalyst contains predominantly metallic Pd in the form of small Pd metal nanoparticles with fcc crystal structure and a small amount of Pd oxide species. During the catalytic reaction, the average local structure around Pd changes, since the coordination number of Pd neighbours in more distant coordination shells in the metal fcc structure is significantly increased, indicating that the average size of Pd metal nanoparticles also increased. On the contrary the coordination numbers of oxygen and Pd neighbours of Pd oxide species significantly decreased and shifted to lower distances, indicating the formation of smaller Pd oxide nanoparticles.

The bimetallic $Pd-Cu/Al_2O_3$ catalysts exhibit significantly different local structure around Pd compared to the monometallic Pd/Al_2O_3 catalyst. In the local Pd neighbourhood there are on average two Cu neighbours at the distance of 2.58 Å and seven Pd neighbours at the distance of 2.70 Å. The Pd-Cu and Pd-Pd distances are in perfect agreement with those reported for the Pd-Cu metal nanoparticles [18]. The fresh bimetallic $Pd-Cu/Al_2O_3$ catalyst contains predominantly Pd-Cu metal alloy nanoparticles and a small amount of Pd oxide species. After the catalytic reaction the average coordination numbers of Cu and Pd neighbours are increased, indicating that the average size of Pd-Cu metal nanoparticles increased. Surprisingly, for the $Pd-Cu/Al_2O_3$ sample, Cu-Pd alloy nanoparticles were formed, while for the Cu and Rh catalyst, no Cu-Rh alloy was formed. The two metals remained separated in similar nanoparticles as in the corresponding monometallic catalysts.

4. Materials and Methods

All reagents and solvent were purchased from Aldrich (Milano, Italy) and used as received. γ-Al_2O_3 type 49 was a generous gift of Chimet S.P.A. (Arezzo, Italy) while 1-(benzo1,3-dioxol-5-yl)propan-1-one was a generous gift of Endura S.P.A. (Bologna, Italy). Helional® was synthetized according to the literature [8]. All the catalysts were prepared following a procedure described below [4]. The metal content was determined by atomic absorption measurements using a Perkin Elmer Analyst 100 spectrometer (Waltham, MA, USA) equipped with a single-element hollow cathode lamp. GLC analyses were carried out with an Agilent 6850A (Santa Clara, CA, USA) equipped with a Free Fatty Acid capillary

column and using isopropyl benzene as an internal standard. GC-MS analyses were performed with an Agilent 7820A GC System coupled with quadrupole mass spectrometer Agilent 5977B MSD (Santa Clara, CA, USA) equipped with a HP-5MS capillary column. Organic products were characterised by ^{1}H NMR spectra recorded in CDCl$_3$ solutions with a Bruker Avance 400 spectrometer (Karlsruhe, Germany) working at 400 MHz. Cu, Rh, and Pd K-edge XANES and EXAFS spectra were measured in transmission detection mode. The experiments were performed at the XAFS beamline of the Elettra synchrotron in Trieste, Italy. Further details are reported in the Supplementary Materials.

4.1. Preparation of Pd/Al$_2$O$_3$

In a glass test tube, 26 mg (0.15 mmol) of PdCl$_2$, 20 mL of cyclopentyl methyl ether (CPME), 0.22 mL (0.50 mmol) of trioctyl amine (TOA), and 5 g of alumina type 49 (Chimet, Arezzo, Italy) were introduced. Three vacuum-nitrogen cycles were then performed. The test tube was placed in a steel autoclave by flushing nitrogen, and subsequently 0.1 MPa of H$_2$ were loaded. The autoclave was maintained at 50 °C under stirring for 24 h, and then the gases were discharged. The grey solid was filtered, under nitrogen, on gooch and washed first with CPME and then with *n*-hexane; the solid was then dried under vacuum. The solid catalyst was analysed to determine the content of Palladium, finding 0.3% Pd/Al$_2$O$_3$. It was stored in a nitrogen atmosphere.

4.2. Preparation of Rh/Al$_2$O$_3$

The catalyst was prepared by using the same protocol above described but starting from 50 mg of RhCl$_3$. The recovered catalyst was dried under vacuum. The solid catalyst was analysed to determine the content of Rhodium, finding 0.18% Rh/Al$_2$O$_3$. The catalyst was stored in a nitrogen atmosphere.

4.3. Preparation of Pd-Cu/Al$_2$O$_3$

In a glass test tube, 12.5 mg (0.0705 mmol) of PdCl$_2$, 27.9 mg (0.282 mmol) of CuCl, 10 mL of cyclopentyl methyl ether (CPME), 0.25 mL of trioctyl amine (TOA), and 2.5 g of alumina type 49 (Chimet) were introduced. Three vacuum-nitrogen cycles were then performed. The test tube was placed in a steel autoclave by flushing nitrogen, and subsequently 0.6 MPa of H$_2$ were loaded. The autoclave was maintained at 50 °C under stirring for 24 h, and then the gases were discharged. The grey solid was filtered, under nitrogen on gooch and washed first with CPME and then with *n*-hexane; the solid was then dried under vacuum. The solid catalyst was analysed to determine the content of Palladium and Copper, finding 0.18% Pd and 0.43% Cu. The catalyst was stored in a nitrogen atmosphere.

4.4. Preparation of Rh-Cu/Al$_2$O$_3$

In a glass test tube, 12.5 mg (0.060 mmol) of RhCl$_3$, 31.8 mg (0.321 mmol) of CuCl, 10 mL of cyclopentyl methyl ether (CPME), 0.56 mL of trioctyl amine (TOA), and 2.5 g of alumina type 49 (Chimet) were introduced. Three vacuum-nitrogen cycles were then performed. The test tube was placed in a steel autoclave by flushing nitrogen, and subsequently 0.6 MPa of H$_2$ were loaded. The autoclave was maintained at 50 °C under stirring for 24 h, and then gases were discharged. The grey solid was filtered, under nitrogen, on gooch and washed first with CPME and then with *n*-hexane; the solid was then dried under vacuum. The solid catalyst was analysed to determine the content of Rhodium and Copper, finding 0.19% Rh and 0.8% Cu. The catalyst was stored in a nitrogen atmosphere.

4.5. Synthesis of 3-(Benzo1,3-dioxol-5-yl)-3-chloro-2-methylacrylaldehyde (**IX**)

The synthesis of (**IX**) was carried out, improving the literature protocol [8]: 20.5 g of *N,N*-dimethylformamide at 0 °C were introduced in a jacketed 3-necked flask equipped with a bubble condenser and then 23 g of POCl$_3$ were added under an inert atmosphere. The mixture was left to react for 2 h after which the temperature was raised to 20 °C for 30 min. Once the temperature was reached, a solution of 14.3 g of 1-(benzo-1,3-dioxol-5-

yl)propan-1-one in *N,N*-dimethylformamide was added over a period of approximately 4 h and left to react overnight at 35 °C. The mixture was cooled to 10 °C; then 35 g of toluene and 95 g of a 3 M NaOH solution were added in 3 h, at a controlled temperature (20 °C) and for a further 2 h at 25 °C. The organic phase was collected and solvent evaporated to give a mixture containing 99.3% of 3-(benzo-1,3-dioxol-5-yl)-3-chloro-2-methylacrylaldehyde (**IX**) and 0.7% 1-(benzo-1,3-dioxol-5-yl)propane as confirmed by GC-MS m/z 3-(benzo1,3-dioxol-5-yl)-3-chloro-2-methylacrylaldehyde (**I**): 224$[M]^+$, 189$[M–Cl]^+$, 161$[M–Cl–CO]^+$. ^{1}H NMR (400 MHz, CDCl$_3$) δ 9.51 (s, 1H), 6.94 (s, 1H), 6.83 (m, 2H), 6.05 (s, 2H), 5.98 (s, 3H).

*4.6. General Procedure for the Hydrodechlorination of 3-(Benzo-1,3-dioxol-5-yl)-3-chloro-2-methylacrylaldehyde (**IX**)*

In a Schlenk tube (glass laboratory of the University) equipped with a magnetic stirring bar, under inert atmosphere, 20 mg (8.9×10^{-2} mmol) of (**IX**), 5 mL of 2-propanol, 2 equivalents of a base, 8.9×10^{-3} mmol of isopropyl benzene as internal standard, and the catalyst were added in the desired amount. The Schlenk tube was then transferred into a 150 mL stainless steel autoclave under nitrogen, pressurized with hydrogen at the desired pressure, and heated at 80 °C for 6 h or 24 h, under stirring. The reactor was then cooled to room temperature and the residual gases vented off. The reaction mixture was centrifuged and the organic solution analysed by GLC and GC-MS. All data were performed in triplicates, and average values are reported in Tables 1 and 2 (see Section 2).

GC-MS *m/z* (E)-3-(benzo-1,3-dioxol-5-yl)-2-methylacrylaldehyde (**X**): 190 $[M]^+$; 175 $[M-CH_3]^+$; 161 $[M-CHO]^+$. GC-MS *m/z* 3-(benzo-1,3-dioxol-5-yl)-2-methylpropanal (Helional$^®$) (**III**): 192 $[M]^+$; 164 $[M–CO]^+$; 135 $[M–CO–C_2H_4]^+$; 121 $[M–CO–C_2H_4–CH]^+$. GC-MS *m/z* 3-(benzo-1,3-dioxol-5-yl)-2-methylpropan-1-ol (**XI**): 194$[M]^+$; 176$[M-H_2O]^+$; 135$[M–CH_3–CH–CH_2OH]^+$.

5. Conclusions

In this paper, different mono- and bimetallic heterogeneous catalysts have been tested for the synthesis of Helional (**III**) by hydrodechlorination of 3-(benzo-1,3-dioxol-5-yl)-3-chloro-2-methylacrylaldehyde (**IX**). In particular, Pd/Al$_2$O$_3$ and Rh/Al$_2$O$_3$ catalysts with low metal loadings (0.3% and 0.18%, respectively) were very efficient, reaching complete substrate conversion. In the presence of Pd/Al$_2$O$_3$ selectivity to (**III**) up to 83% were obtained in the presence of 2 equivalents of TEA, at 80 °C, p(H$_2$) 0.5 MPa by 24 h. When Rh/Al$_2$O$_3$ was chosen as a catalyst, although a higher p(H$_2$) (1.0 MPa) was employed, total conversion of (**IX**) and very high selectivity to (**III**) (99%) were achieved by 24 h, thus giving better results in comparison with data reported in the literature [11]. Hydrodechlorination tests carried out in the presence of bimetallic Pd-Cu/Al$_2$O$_3$ and Rh-Cu/Al$_2$O$_3$ catalysts showed that these catalysts have very lower performances compared to monometallic Pd/Al$_2$O$_3$ and Rh/Al$_2$O$_3$ catalysts.

To investigate the possible correlation between the atomic structure of the catalysts and the chemical state and atomic structure of the Cu, Rh, and Pd cations on the alumina support, all the catalytic systems have been characterized by Cu, Rh, and Pd K-edge XANES, EXAFS analysis [15–18].

The bimetallic Pd-Cu/Al$_2$O$_3$ catalysts exhibit significantly different local structure around Pd compared to the monometallic Pd/Al$_2$O$_3$ catalyst. The monometallic Pd/Al$_2$O$_3$ catalyst contains predominantly metallic Pd in the form of small Pd metal nanoparticles with fcc crystal structure while bimetallic Pd-Cu/Al$_2$O$_3$ catalysts contain predominantly Pd-Cu metal alloy nanoparticles, hindering the catalytic activity of Pd. In fact, from these characterisations it emerged that the addition of Cu reduces the amount of catalytically active Pd sites by formation of Pd-Cu alloy nanoparticles. Additionally, the excess of Cu cations forms on alumina surface a mixture of Cu metal nanoparticles with fcc crystal structure and Cu oxide/hydroxide nanoparticles, which are catalytically not active.

In the case of Rh-based catalysts, both the monometallic Rh/Al$_2$O$_3$ and bimetallic Rh-Cu/Al$_2$O$_3$ contain Rh cations predominantly in the form of Rh oxide species and a

small amount of metallic Rh. The main structural difference in the bimetallic catalyst is represented by the presence of Cu(II) oxide/hydroxide species highly dispersed and tightly attached on the surface of Al_2O_3. As for Pd-Cu/Al_2O_3, the Cu species are catalytically not active and thus hinder the performance of the Rh active sites present on the surface of the Al_2O_3 support.

The XANES and EXAFS analysis also revealed structural changes and degradation of the catalyst after use, diminishing their catalytic performances. In the case of the monometallic Rh/Al_2O_3 and bimetallic Rh-Cu/Al_2O_3, the reason can be attributed to nanoparticles formation and loss of the direct tight connection of the remaining Cu(II) oxide/hydroxide species to the alumina support. In the case of the mono-metallic Pd/Al_2O_3 and bimetallic Pd-Cu/Al_2O_3 catalyst, the average size of Pd and Pd-Cu metal nanoparticles, increased during the catalytic reaction, decreasing the catalyst efficiency. Studies are ongoing to gain deeper insight into the different behaviours of mono- and bimetallic catalysts and the role of alloys formed during the reaction.

References

1. Bartolomew, C.H.; Farrauto, R.J. *Fundamentals of Industrial Catalytic Processes*, 2nd ed.; John Wiley and Sons: Hoboken, NJ, USA, 2006.
2. Piccolo, O.; Verrazzani, A. Preparation and Use of a Heterogeneous Rhodium Catalyst for the Hydrogenation of a Double Bond of an Alpha-Beta-Unsaturated Carbonyl Compound. U.S. Patent 7087548, 8 August 2006.
3. Paganelli, S.; Tassini, R.; Rathod, V.D.; Onida, B.; Fiorilli, S.; Piccolo, O. A low rhodium content smart catalyst for hydrogenation and hydroformylation reactions. *Catal. Lett.* **2021**, *151*, 1508–1521. [CrossRef]
4. Paganelli, S.; Angi, A.; Pajer, N.; Piccolo, O. A smart heterogeneous catalyst for efficient, chemo- and stereoselective hydrogenation of 3-hexyn-1-ol. *Catalysts* **2021**, *11*, 14. [CrossRef]
5. Kraft, P.; Bajgrowicz, J.A.; Denis, C.; Frater, G. Odds and Trends: Recent Developments in the Chemistry of Odorants. *Angew. Chem. Int. Ed.* **2000**, *39*, 2980–3010. [CrossRef]
6. Wenxiang, L. Synthesis of helional from piperonylenepropanal. *Huaxue Yanjiu Yu Yingyong* **2004**, *16*, 417.
7. Beets Muus Gerrit, J.; van Essen, H. 2-Piperonyl-Propanal, a New Perfume, and Process for Making Same. GB841921, 20 July 1960.
8. Takashi, D.; Yoshida, Y.; Eiji, S.; Satoru, F. 2-Methyl-3-(3,4-methylenedioxyphenyl)propanal, and Method for Production Thereof. EP2119713A1, 18 November 2009.
9. Yoshida, Y.; Doi, T. Development of new environmentally benign process for marine fragrance (Heliofresh). *Fain Kemikaru* **2013**, *42*, 14–19.
10. Doi, T.; Yoshida, Y.; Sajiki, E.; Fujitsu, S. Method of Retaining the Quality of 2-methyl-3-(3,4-methylenedioxyphenyl)propanal and Process for Producing the Same. WO2008108429A1, 12 September 2008.
11. Borzatta, V.; Capparella, E.; Poluzzi, E. Process for the Preparation for 3-(3,4-methylenedioxyphenyl)-2-methylpropanal. WO2005/105774 A1 10 November 2005.
12. Fang, D.; Li, W.; Zhao, J.; Liu, S.; Ma, X.; Xu, J.; Xia, C. Catalytic hydrodechlorination of 4-chlorophenol over a series of Pd–Cu/γ-Al$_2$O$_3$ bimetallic catalysts. *RSC Adv.* **2014**, *4*, 59204–59210. [CrossRef]
13. Bosello, N.; Di Michele, A.; Piccolo, O.; Paganelli, S. CO and H$_2$ gas-free efficient reductive carbonylation of aryl iodides. Use of smart recyclable metal-based catalysts. *Appl. Catal. A Gen.* **2023**, *657*, 119145. [CrossRef]
14. Ravel, B.; Newville, M. Athena, Artemis, Hephaestus: Data analysis for X-ray absorption spectroscopy using IFEFFIT. *J. Synchrotron Radiat.* **2005**, *12*, 537–541. [CrossRef] [PubMed]
15. Rehr, J.J.; Albers, R.C.; Zabinsky, S.I. High-order multiple-scattering calculations of X-ray absorption fine structure. *Phys. Rev. Lett.* **1992**, *69*, 3397–3400. [CrossRef] [PubMed]
16. Myers, S.V.; Frenkel, A.I.; Crooks, R.M. X-ray Absorption Study of PdCu bimetallic alloy nanoparticles containing an average of ∼64 atoms. *Chem. Mater.* **2009**, *21*, 4824–4829. [CrossRef]
17. Kroner, A.B.; Newton, M.A.; Tromp, M.; Russell, A.E.; Dent, A.J.; Evans, J. Structural characterization of alumina-supported Rh catalysts: Effects of ceriation and zirconiation by using metal-organic precursors. *ChemPhysChem* **2013**, *14*, 3606–3617. [CrossRef] [PubMed]
18. Waser, J.; Levy, H.A.; Peterson, S.W. The structure of PdO. *Acta Crystallogr.* **1953**, *6*, 661–663. [CrossRef]
19. Di Cicco, A.; Aquilanti, G.; Minicucci, M.; Principi, E.; Novello, N.; Cognigni, A.; Olivi, L. Novel XAFS capabilities at Elettra synchrotron light source. *J. Phys. Conf. Ser.* **2009**, *190*, 012043. [CrossRef]
20. Zabilskiy, M.; Arčon, I.; Djinović, P.; Tchernychova, E.; Pintar, A. In-situ XAS study of catalytic N$_2$O decomposition over CuO/CeO$_2$ catalysts. *ChemCatChem* **2021**, *13*, 1814–1823. [CrossRef]
21. Gogate, M.R.; Davis, R.J. X-ray Absorption Spectroscopy of a Fe-promoted Rh/TiO$_2$ catalyst for synthesis of ethanol from synthesis gas. *ChemCatChem* **2009**, *1*, 295–303. [CrossRef]
22. Arčon, I.; Paganelli, S.; Piccolo, O.; Gallo, M.; Vogel-Mikuš, K.; Baldi, F. XAS analysis of iron and palladium bonded to a polysaccharide produced anaerobically by a strain of Klebsiella Oxytoca. *fACS Appl. Mater. Interfaces* **2023**, *22*, 1215.
23. Žumbar, T.; Arčon, I.; Djinović, P.; Aquilanti, G.; Žerjav, G.; Pintar, A.; Ristić, A.; Dražić, G.; Volavšek, J.; Mali, G.; et al. Winning combination of Cu and Fe Oxide clusters with an alumina support for low-temperature catalytic oxidation of volatile organic compounds. *ACS Appl. Mater. Interfaces* **2023**, *15*, 28747–28762. [CrossRef] [PubMed]
24. Christy, A.G.; Clark, S.M. Structural behavior of palladium (II) oxide and a palladium suboxide at high pressure: An energy-dispersive X-ray diffraction study. *Phys. Rev. B* **1995**, *52*, 9259–9265. [CrossRef] [PubMed]

25. Saraev, A.A.; Yashnik, S.A.; Gerasimov, E.Y.; Kremneva, A.M.; Vinokurov, Z.S.; Kaichev, V.V. Atomic structure of Pd-, Pt-, and PdPt-Based catalysts of total oxidation of methane: In situ EXAFS study. *Catalysts* **2021**, *11*, 1446. [CrossRef]
26. Muravev, V.; Simons, J.F.M.; Parastaev, A.; Verheijen, M.A.; Struijs, J.J.C.; Kosinov, N.; Hensen, E.J.M. Operando spectroscopy unveils the catalytic role of different palladium oxidation states in CO oxidation on Pd/CeO$_2$ catalysts. *Angew. Chem. Int. Ed.* **2022**, *61*, e202200434. [CrossRef] [PubMed]